

Supplementary Materials for
Cumulative risk of future bleaching for the world's coral reefs

Camille Mellin *et al.*

Corresponding author: Camille Mellin, camille.mellin@adelaide.edu.au.

Sci. Adv. **10**, eadn9660 (2024)
DOI: 10.1126/sciadv.adn9660

This PDF file includes:

Supplementary Text
Figs. S1 to S10
Table S1

Supplementary Text

Ecological validation

Overall, the *ens5* multi-model ensemble predicted past bleaching records with higher accuracy than the satellite-based CCI analysis SST ($X^2(1) = 9.09$, $p = 0.002$). A region-level analysis indicated that *ens5* was better able to predict the number of individual bleaching records in 5 of the 18 regions that had >10 bleaching records recorded (Caribbean $X^2(1) = 5.88$, $p = 0.015$; South East Asia $X^2(1) = 3.89$, $p = 0.048$; Southern Pacific Ocean $X^2(1) = 18.58$, $p < 0.001$; Eastern Australia $X^2(1) = 11.43$, $p < 0.001$; South East Africa $X^2(1) = 4.16$, $p < 0.04$) (Fig. S4). However, when comparing across all regions (i.e., globally), there was no statistical support that the *ens5* ensemble could more, or less, accurately predict the total number of regional scale bleaching records when compared to the CCI analysis SST ($V = 56$, $p = 0.552$). We found a mean hit rate of 90% (S.D. = 13%) across the IPCC AR6 regions from the *ens5* projections (Fig. S4A), compared to a mean hit rate of 92% (S.D. = 13%) from the CCI analysis SST (Fig. S4B).

Bayesian beta-regression indicated that the neither the *ens5* data nor the CCI analysis SST performed better in the 18 regions with higher numbers (>10) of bleaching records. No clear relationship was apparent between the number of bleaching records and the proportional hit-rate across regions (*ens5* = 0.05, 95% CI -0.31:0.46; CCI analysis SST = -0.07 95% CI -0.41:0.33). All posterior model checks, including the Gelman-Rubin statistic, effective sample size, and traceplots, indicated that the models were constructed correctly and showed no evidence of lack of convergence or autocorrelation.

The *ens5* model had improved performance over individual CMIP6 models in all IPCC AR6 regions (Fig. S5A). Individual model skill varied greatly between regions, with some regions such as the North Pacific Ocean (NPO) and South Pacific Ocean (SPO) showing reduced skills in all models, including the satellite monitoring data, as well as greater hit rate variability (Fig. S5B).

DHW values during the baseline period showed similar distributions (mostly < 1°C-week) for the *ens5* hindcast and the CCI analysis SST (Fig. S6). In each case they were distinct from the distribution of DHW values matching severe bleaching records, suggesting that both datasets enable the distinction of baseline from bleaching conditions.

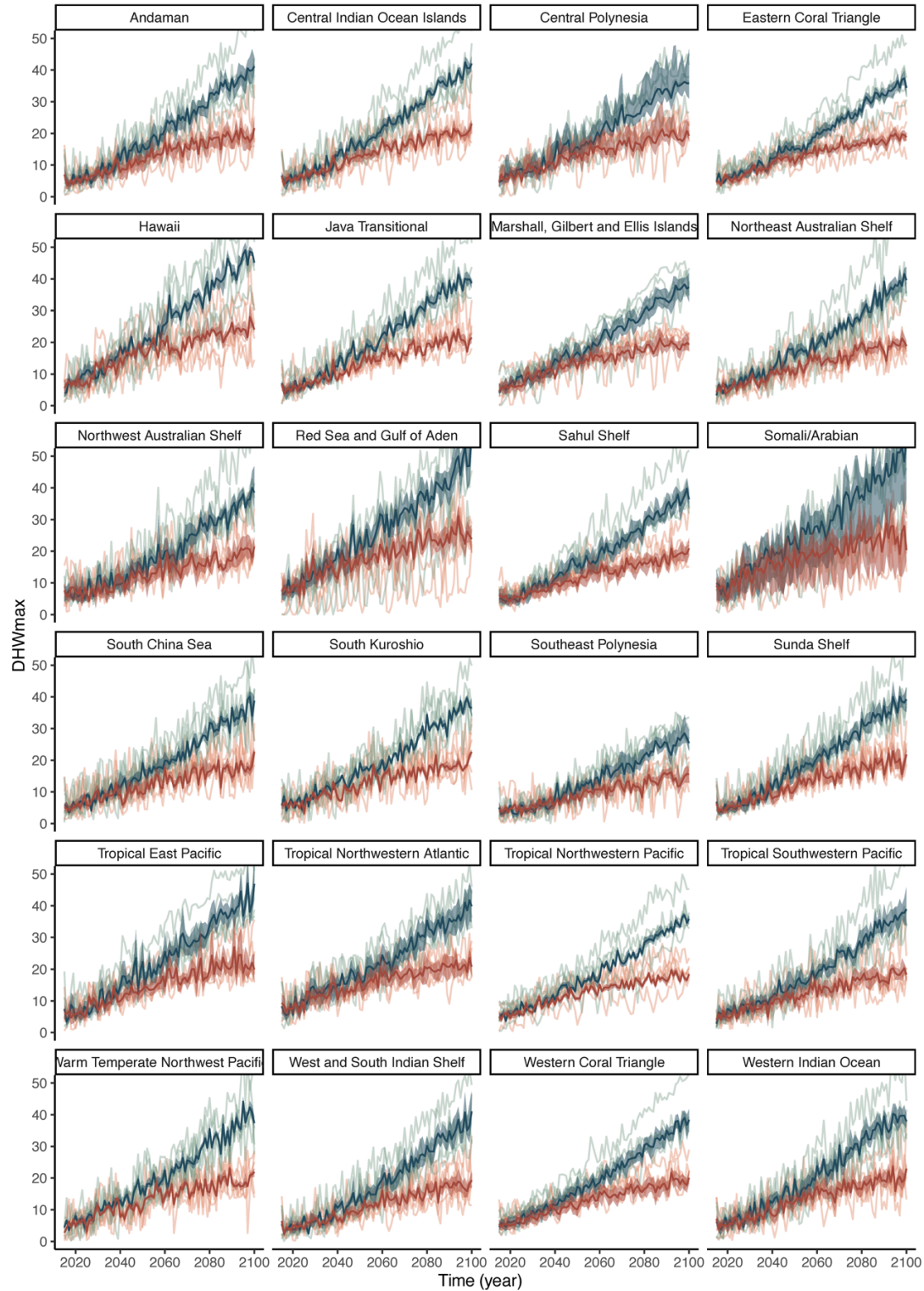
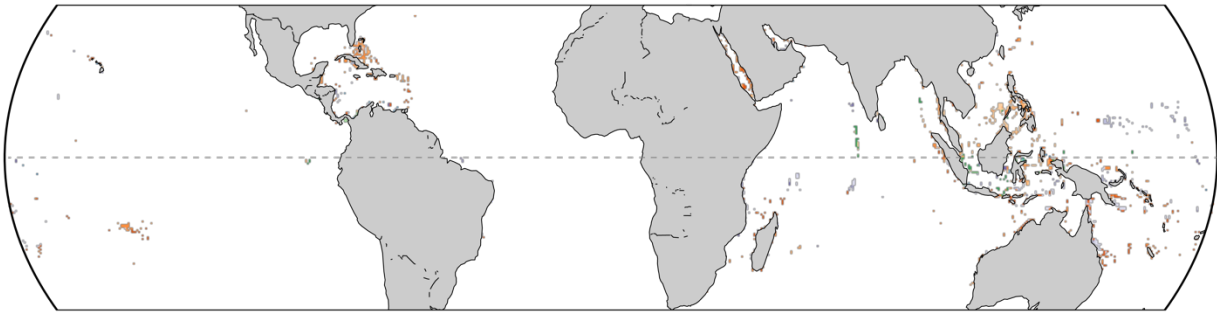


Fig. S1. Annual maximum Degree Heating Weeks (DHWmax; °C-week) trajectories based on the 5-model ensemble (*ens5*) and according to two climate scenarios (SSP2-4.5 and SSP5-8.5) in each marine ecoregion. Individual climate models are shown as thin lines, and the five-model ensemble is shown as the thick line, with 95% confidence interval shown as the ribbon.

A- 5-model ensemble



B- Satellite analysis

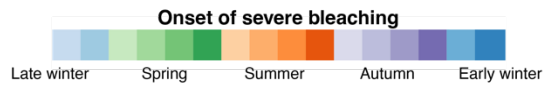
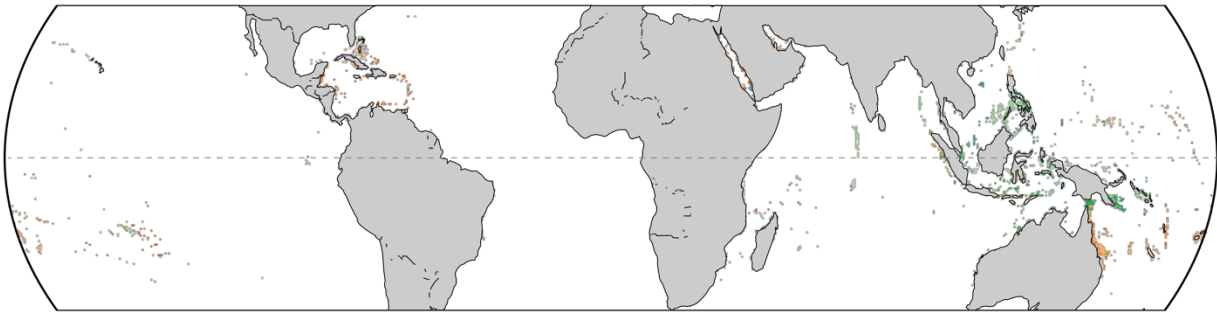


Fig. S2. Baseline climatology for onset of severe bleaching conditions predicted within reef grid cells in 2000 (i.e., averaged across 1985-2015) according to (A) the *ens5* multi-model ensemble, and (B) satellite analysis (28). Bleaching onset is defined as the number of days since mid-winter when Bleaching Alert 1 first occurs in each grid cell ($DHW \geq 4^{\circ}\text{C}\text{-week}$).

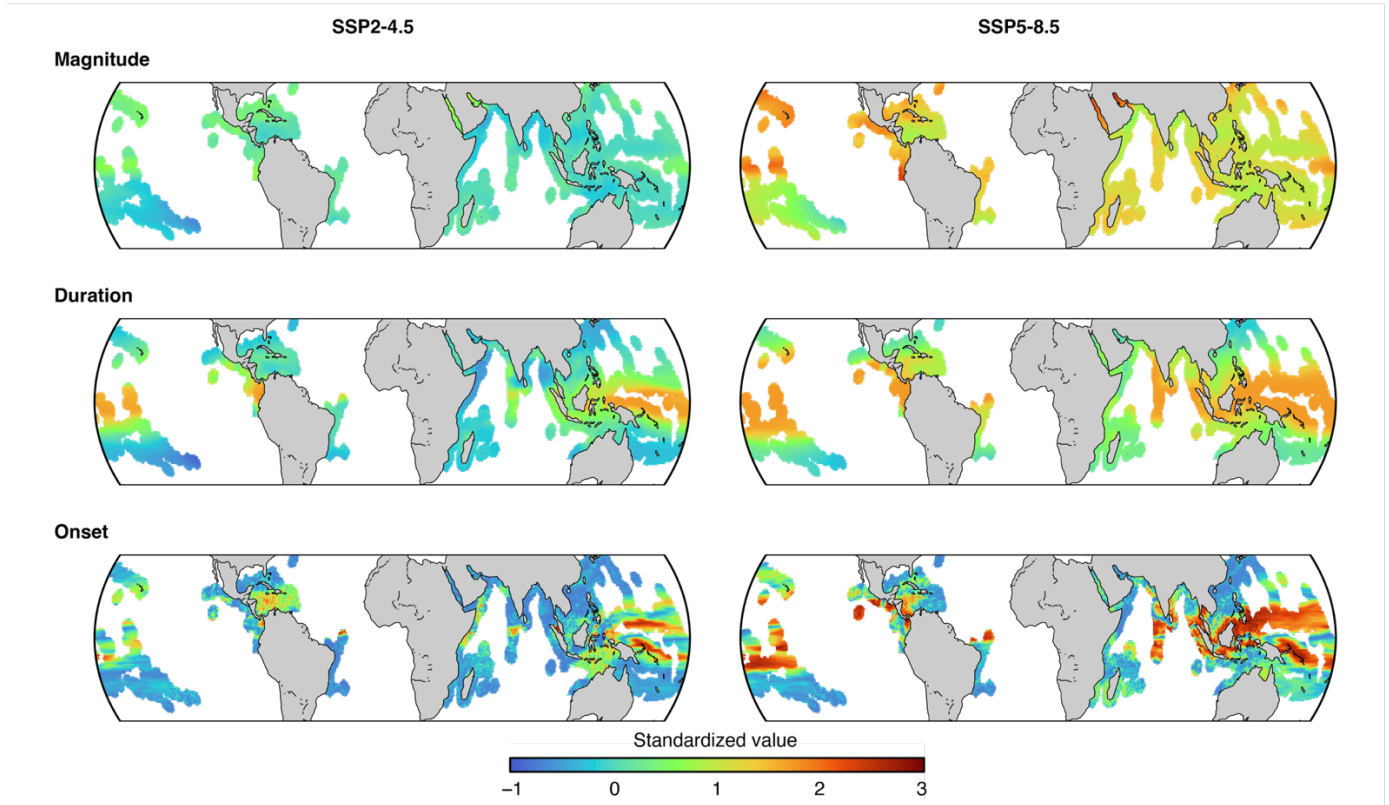


Fig. S3. Spatial patterns in heat stress magnitude, duration and onset projected for 2080 under climate scenarios SSP2-4.5 and SSP5-8.5. All values are standardized by subtracting the mean and dividing by the standard deviation for easier comparison.

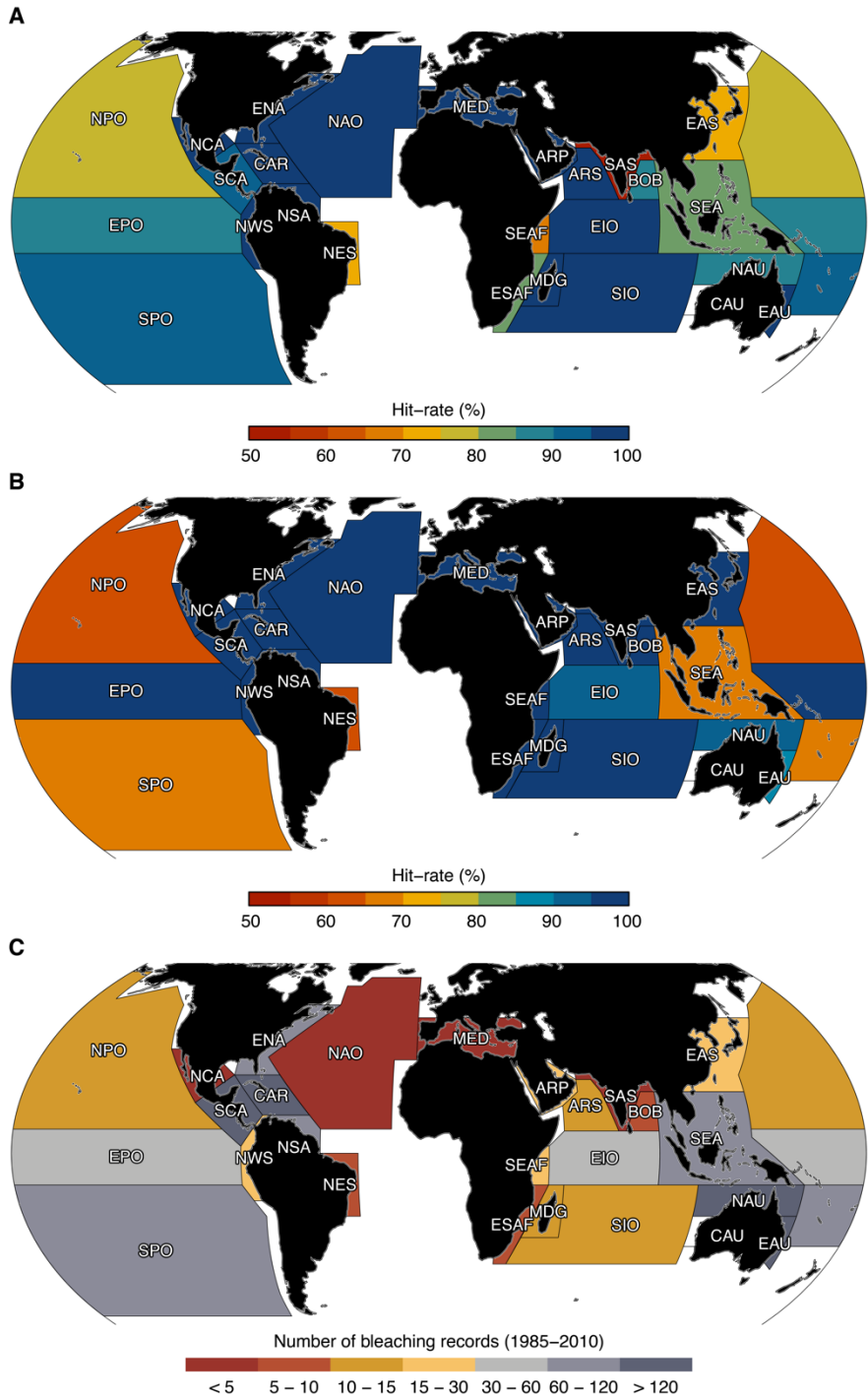


Fig. S4. Ecological validation of the ensemble model projections in IPCC AR6 regions between 1985 and 2010 for (A) the 5-model ensemble (*ens5*) and (B) the satellite-based CCI analysis SST. (C) shows the number of severe bleaching records in each IPCC AR6 region (total = 1,975) (7). The hit rate quantifies the proportion of observed severe bleaching records that were accurately predicted by the models (i.e., where the model ensemble predicted a Bleaching Alert Level 1 or above; $DHW \geq 4^{\circ}\text{C}\text{-week}$).

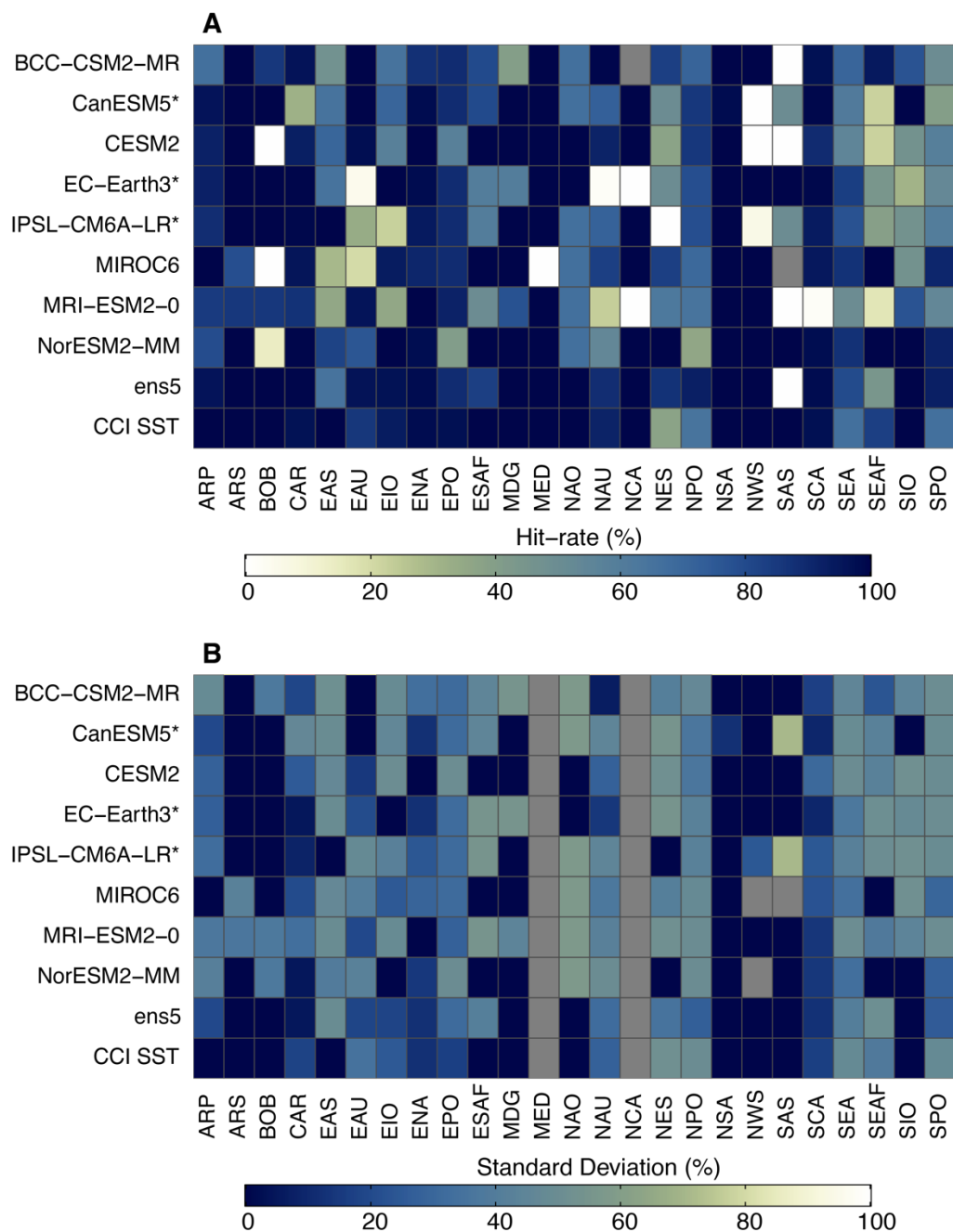


Fig. S5. Ecological validation of the individual climate models across IPCC AR6 regions: Assessment of the ability of the downscaled and bias-corrected CMIP6 models to effectively predict observed coral bleaching records in IPCC AR6 regions measured as (A) mean % hit-rate and (B) % hit rate standard error (S.E.). CMIP6 models (individual models and 5-model average, *ens5*) and the CCI analysis SST are shown as rows, with IPCC AR6 regions shown as columns (see Fig. S4 for region locations). Models not selected for *ens5* are indicated by asterisks (*).

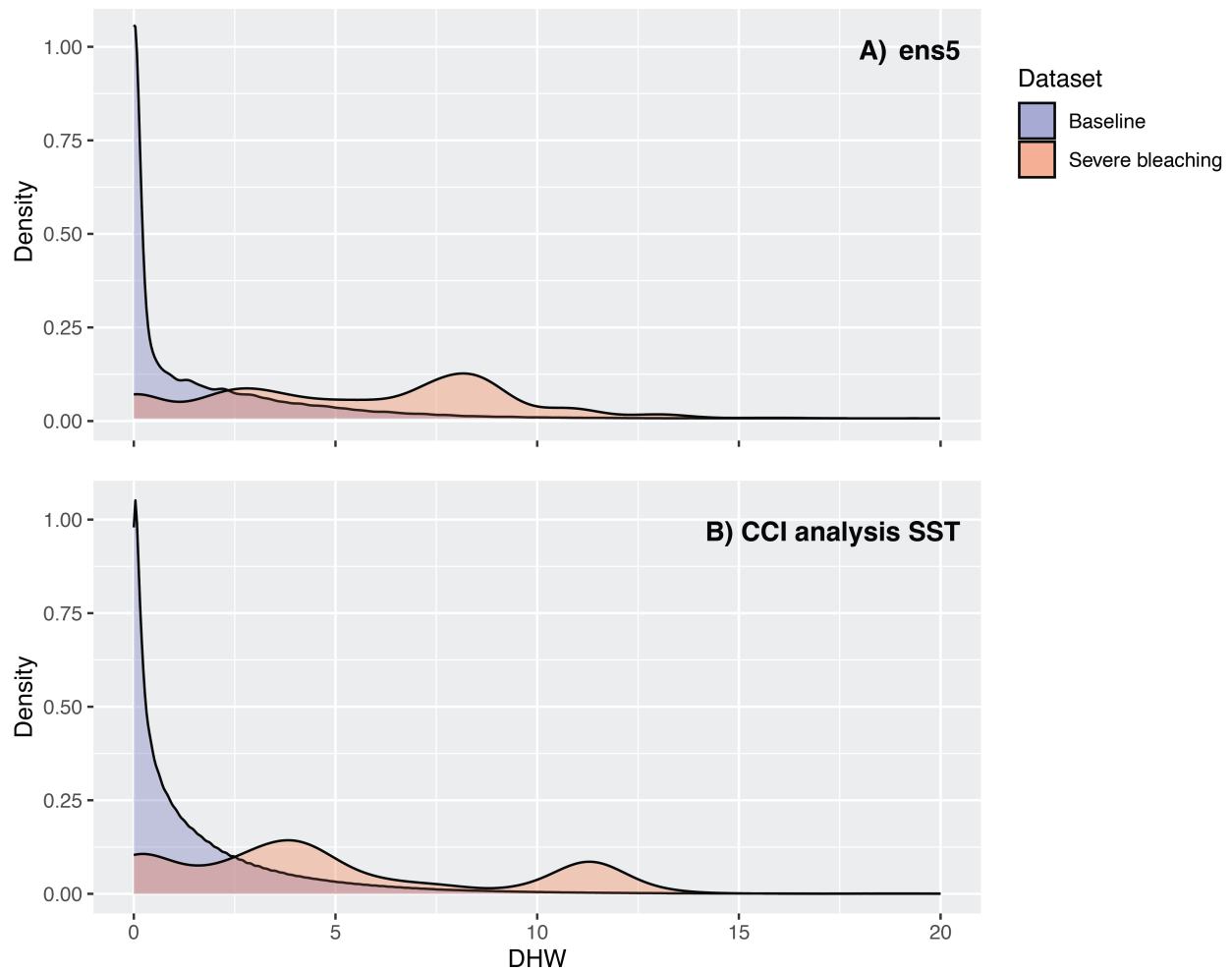


Fig. S6. Distribution of DHW corresponding to severe bleaching records and throughout the climatological baseline period. Density plots show DHW distributions only during severe bleaching records within 1985-2012 (red) and throughout the baseline period (i.e., all days considered between 1985-2012 at the same locations; blue) for (A) the *ens5* multi-model ensemble and (B) the CCI analysis SST.

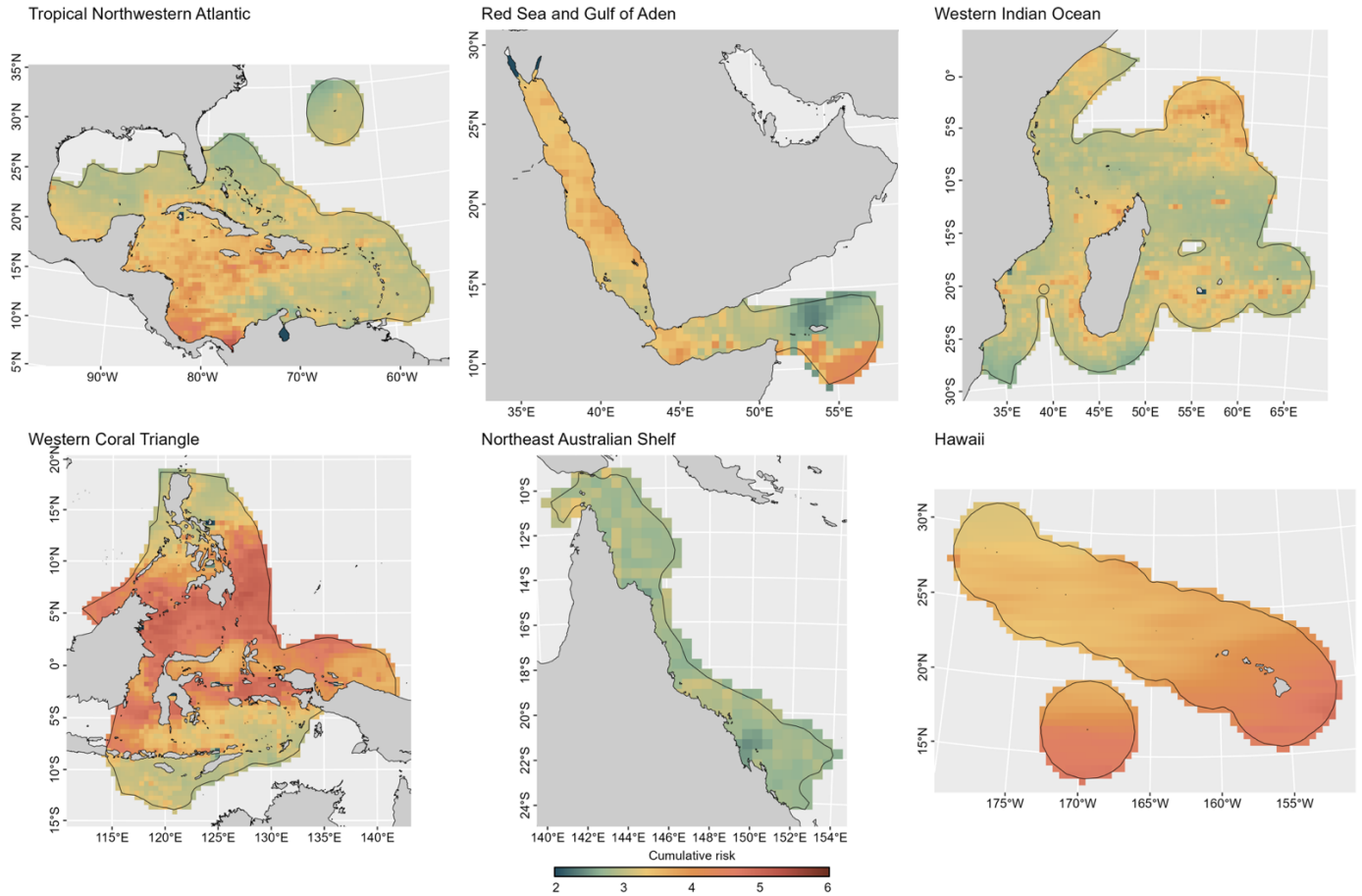


Fig. S7. Regional patterns in cumulative risk of future coral bleaching projected in 2080 within six major coral reef provinces: (i) Tropical Northwestern Atlantic, (ii) Red Sea and Gulf of Aden, (iii) Western Indian Ocean, (iv) Western Coral Triangle, (v) Northeast Australia Shelf and (vi) Hawaii. Province boundaries are defined based on the Marine Ecoregions Of the World classification (61).

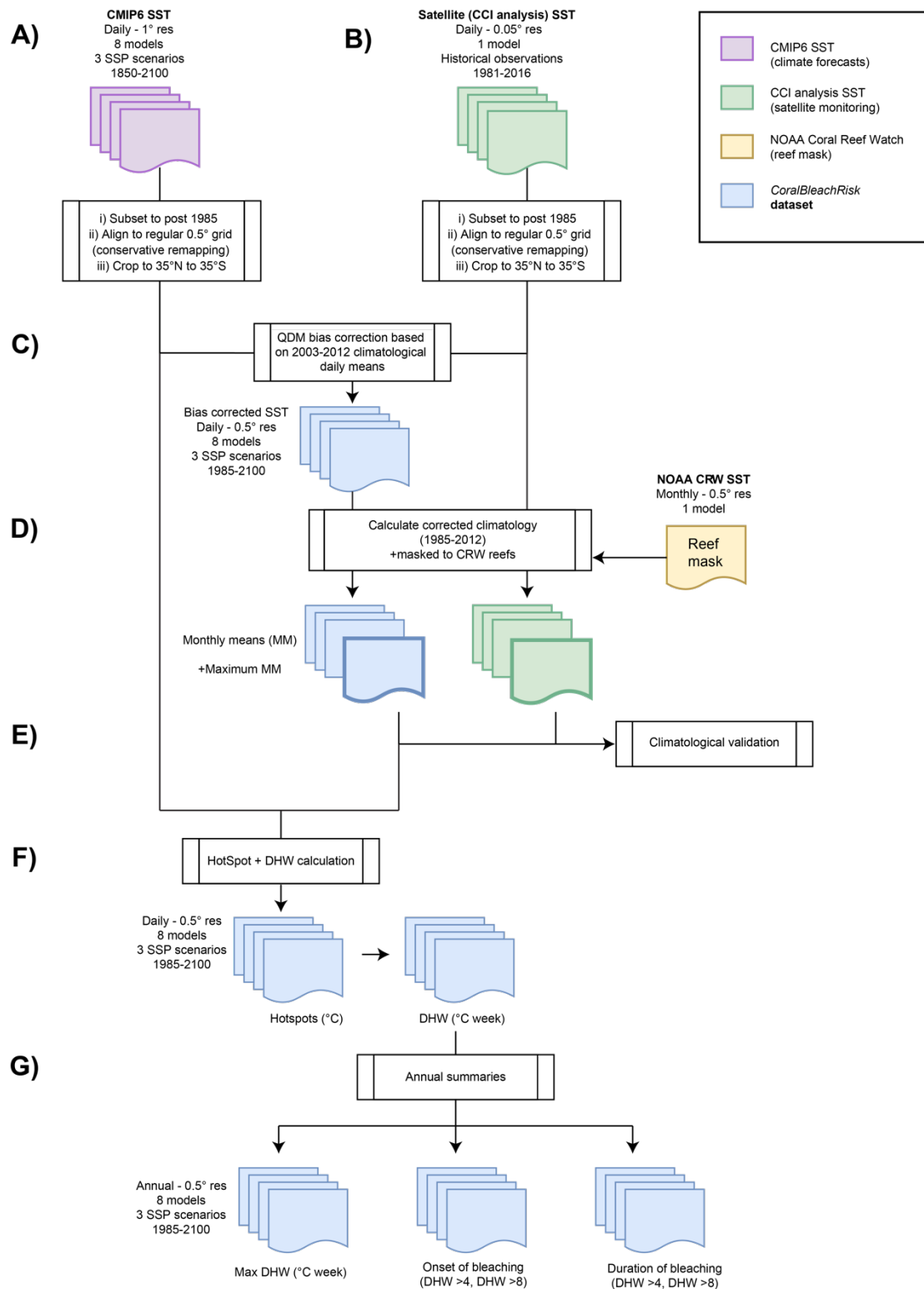


Fig. S8. Schematic overview of the processing steps and design of the CoralBleachRisk database, adapted from Mellin et al. (39). (A) Simulated projections of sea-surface temperatures (SST) from historical and future climates were extracted from eight CMIP6 climate models for

the period 1985 to 2100. (B) Satellite observations of SSTs (1985 to 2016) were extracted from the CCI analysis SST. Both datasets were re-gridded to a common $0.5^\circ \times 0.5^\circ$ resolution. (C) CMIP6 projections were bias corrected against the CCI analysis SST data using quantile delta mapping (QDM). (D) Climatological monthly mean SST were calculated from the downscaled and bias corrected CMIP6 projections and CCI analysis data. (E) CMIP6 projections of mean monthly SST were validated against CCI analysis data from 1985 to 2014. (F) Hotspots ($^\circ\text{C}$) and Degree Heating Weeks (DHW, $^\circ\text{C}\text{-week}$) were calculated for each pixel at a daily resolution between 1985 and 2100. (G) Daily DHW data were used to calculate annual measures (heat stress magnitude, duration, onset) of severe bleaching risk in each pixel. These projections were validated against global observations of coral bleaching for the period 1985-2012 (7).

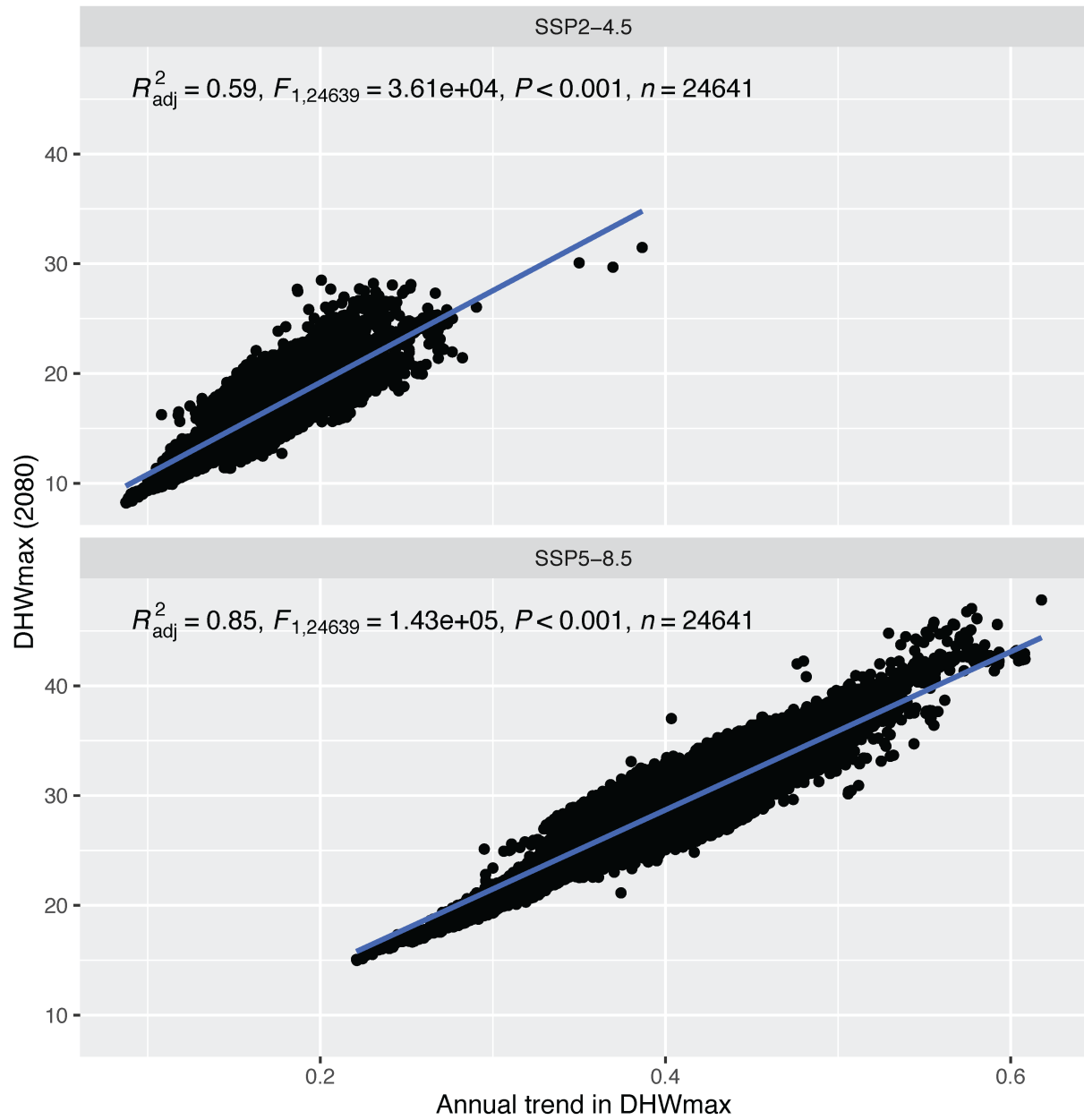


Fig. S9. Relationship between DHW_{max} in 2080 and Sen's slope calculated over the 2015-2100 time period for each climate scenario.

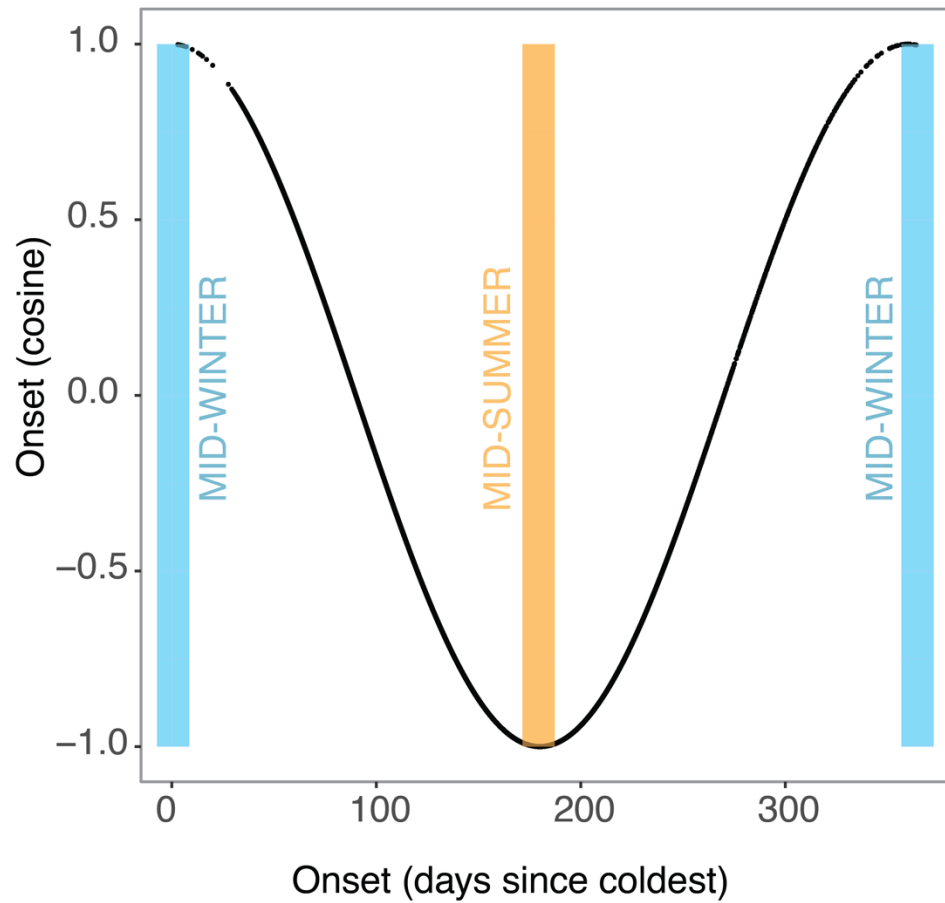


Fig. S10.

Cosine transformation of the onset of coral bleaching conditions for input in the principal component analysis. Raw onset values are shown on the x-axis, cosine-transformed ones on the y-axis. An onset of 0, equivalent to 365 days, represents bleaching conditions beginning in mid-winter; both correspond to a cosine-transformed onset of 1. An onset of 187 days (mid-summer) corresponds to a cosine-transformed onset of -1.

Table S1.

Description of the eight AOGCMs used in our study. All Atmosphere-Ocean General Circulation Models (AOGCMs) had daily data available for the historical period (1850-2014) and three SSP scenarios (SSP2-4.5, SSP3-7.0, SSP5-8.5; 2015-2100). All models had a native nominal resolution of $1^\circ \times 1^\circ$ and were re-gridded from their native non-regular grids to a regular $0.5^\circ \times 0.5^\circ$ grid spanning 35°S to 35°N using quantile delta mapping. ECS = equilibrium climate sensitivity; change in global-mean air temperature due to an instantaneous doubling of CO_2 . TCR = transient climate response; warming from a simulation that is driven by an exponential 1.0 % per year increase in CO_2 . Models with a TCR inside the 1.4-2.2°C range (marked with an asterisk) are those included in the 5-model ensemble (*ens5*) as recommended (57).

Model	Institution(s)	Ocean model	ECS	TCR
<i>BCC-CSM2-MR</i>	Beijing Climate Center	MOM4-L40v2	3.02	*1.59
<i>CanESM5</i>	Canadian Centre for Climate Modelling and Analysis	NEMO-v3.4.1	5.64	2.66
<i>CESM2</i>	National Center for Atmospheric Research	POP2	5.15	*2.04
<i>EC-Earth3</i>	EC-Earth consortium	NEMO-v3.6	4.26	2.38
<i>IPSL-CM6A-LR</i>	L'Institut Pierre-Simon Laplace	NEMO-v3.6	4.70	2.32
<i>MIROC6</i>	Center for Climate System Research, the University of Tokyo, the Japan Agency for Marine-Earth Science and Technology, the National Institute for Environmental Studies	COCO-v4.5	2.60	*1.52
<i>MRI-ESM2-0</i>	Meteorological Research Institute	MRI.COM-v4	3.13	*1.56
<i>NorESM2-MM</i>	Norwegian Climate Consortium	BLOM	2.49	*1.33